Rotational Spectroscopic and *Ab Initio* Investigation of the Rotamer Geometries of 2-Fluoroanisole and 3-Fluoroanisole

Katrina Bergmann and Jennifer van Wijngaarden*

Department of Chemistry, University of Manitoba, Winnipeg, Manitoba, R3T 2N2, Canada

*Corresponding author

Email: vanwijng@cc.umanitoba.ca

Phone: (204)474-8379

Fax: (204)474-7608

ABSTRACT

The rotational spectra of 2-fluoroanisole (2-FA) and 3-fluoroanisole (3-FA) were investigated using Fourier transform microwave (FTMW) spectroscopy in the 4-26 GHz range. Assigned transitions correspond to the lowest energy rotamer for 2-FA which has the O-CH_3 group directed away (*anti*) from the fluorine substituent whereas for 3-FA, the spectrum is consistent with the presence of two rotamers arising from *syn* and *anti* orientations of the methoxy moiety relative to fluorine. *Ab initio* calculations at the MP2/cc-pVTZ level were used to estimate the equilibrium (r_e) geometries of the three observed rotamers. Their assignments were confirmed through the observation of the rotational transitions of eight minor isotopologues (^{13}C and ^{18}O) in natural abundance for each species. The mass dependence ($r_m^{(1)}$) structures derived using the experimentally determined rotational constants compare favourably with the *ab initio* estimates. The resulting sets of geometric parameters suggest that the aromatic ring backbone is distorted by the introduction of the angular methoxy substituent, with a tendency to induce bond length alternation around the ring, and by the electron withdrawing effects of fluorine.

INTRODUCTION

Rotational spectroscopy is a well-established technique for structural elucidation as the pattern of observed transitions is intrinsically dependent on the geometry of the molecule through its moments of inertia.[1] As experimental techniques in this field have evolved over the past decades to improve sensitivity, resolution and the speed with which rotational spectra are collected, the complexity of molecular systems that can be 'routinely' studied has also expanded. With the support of modern computational methods, accurate experimental geometries can now be derived for the heavy atom frameworks of a vast array of interesting compounds provided transitions due to multiple minor isotopologues are accessible.[2–5] A few recent examples that demonstrate the scope of species whose geometries were derived via rotational spectroscopy include weakly bound complexes,[6,7] mixtures of conformers[8,9] and molecules undergoing internal tunneling motions.[10,11]

In addition to characterizing the overall structures of increasingly complex molecules, modern high resolution Fourier transform microwave (FTMW) spectroscopy has proved invaluable for probing very subtle geometric changes that accompany the addition of a substituent in an organic compound. For example, the fluorinated ring compounds of benzene,[12–14] pyridine,[15,16] and cyanobenzene,[17] have served as simple prototypes in building a detailed understanding of the influence of fluorine on the ring geometry while studies of fluorinated phenol,[18] thiophenol,[19] and benzaldehyde[20] have extended this to also include the impact of

fluorine on intramolecular interactions and conformer distributions. In these ring compounds, the largest geometric changes induced by fluorination are found in close proximity to the substitution site and typically involve an increase in the ring angle at that site by 3-4^{o} and a shortening of the adjacent C-C bonds by 0.005-0.010 Å.

The fluorinated analogs of anisole described herein, provide the opportunity to investigate how the strong electron withdrawing fluorine substituent influences the electronic structure around the entire aromatic ring. The geometry of anisole itself, derived from its rotational spectrum,[21] provided experimental confirmation of the so-called AGIBA (Angular Group Induced Bond Alternation) effect that was first proposed from quantum chemical calculations.[22,23] This phenomenon predicts that when angular functional groups (e.g. methoxy, formyl, vinyl) are added to benzene, the substituent induces a C-C bond length alternation in the ring through stabilization of one Kekulé structure over another. In anisole, for example, the $r_m^{(1)}$ experimental geometry[21] derived from microwave and millimeterwave transitions is shown in Figure 1 and reveals an alternation in the C-C bonds of ~0.01 Å when one compares pairs of bonds that are equidistant from the angular group (e.g. C1-C2 < C6-C1, C2-C3>C5-C6, etc.). In this case, the single O-CH_3 bond in the methoxy substituent lies *anti* to a longer bond, i.e. a bond that is more single bond in character, in the aromatic ring. For comparison, the predicted bond length alternation in

benzaldehyde with the angular formyl group is smaller (0.002-0.004 Å)[21] and could not be spectroscopically confirmed as the experimental uncertainties in the bond lengths were larger in magnitude than the expected AGIBA effect. The $r_m^{(1)}$ experimental geometries derived for 2-fluoro- and 3-fluorobenzaldehyde[20] faced similar limitations but the addition of fluorine to anisole, as in the present study, affords the opportunity to explore whether the electron withdrawing fluorine substituent enhances or reduces the size of the AGIBA effect in comparison to that established for the parent compound.[21]

With fluorine substitution in the *ortho* or *meta* position relative to the methoxy group, rotational isomerism is introduced with the possibility of the methoxy substituent oriented toward (*syn*) or away (*anti*) from fluorine. The infrared and Raman spectra of 3-fluoroanisole (3-FA) recorded in the liquid phase, first confirmed the presence of two rotamers with the *anti* orientation deemed to be more stable by 2.4(6) kJ mol^{-1}.[24] This was the reverse order to that later predicted from ^{1}H NMR studies and *ab initio* calculations (HF: STO-3G, 6-31G) which found the *syn* species

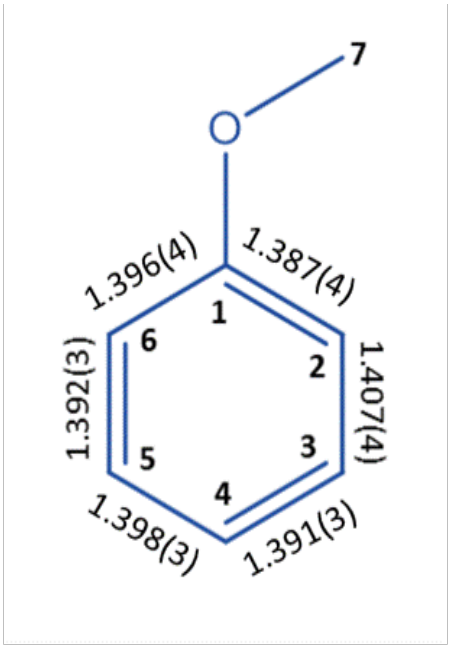

Figure 1: The $r_m^{(1)}$ geometry of anisole showing bond length alternation.[21]

to be lower in energy by 0.45 – 0.85 kJ mol^{-1}.[25] Gas phase electron diffraction (GED) data and results from density functional theory (B3LYP/cc-pVTZ) also indicated that *syn* is the more stable rotamer by 0.46 kJ mol^{-1}.[26] In the microwave region, however, only transitions for the higher energy *anti* isomer were reported in the gas phase at room temperature.[27] The observed spectrum was assigned to rotational transitions in the ground and first three excited torsional states of the parent isotopologue of the *anti* rotamer. The absence of features attributable to the *syn* rotamer was not addressed but estimates of its a- and b-dipole components based on a model derived from extrapolation using the geometries of anisole and fluorobenzene suggested that the intensities of transitions for this form would be only 15-20% the intensity of those of the *anti* rotamer.

For 2-fluoroanisole (2-FA), in contrast, only bands consistent with the *anti* rotamer were initially observed in the infrared and Raman spectra of the liquid and the authors suggested that the *syn* rotamer was destabilized by steric effects between the methoxy and fluorine substituents.[24] Later, a second rotational isomer was reported from GED measurements and was attributed to a nonplanar (np) form with C_2-C_1-O-C_7 dihedral angle of 57(8)º. The ratio of the two forms was estimated to be 70:30 (anti:np).[28] This was consistent with the accompanying MP2 (6-31G*) and B3LYP (6-31G*) predictions which placed the np rotamer 2.13 kJ mol^{-1} (MP2) and 3.89 kJ mol^{-1} (B3LYP) higher in energy than the *anti* form. The presence of the np rotamer was subsequently confirmed by Isozaki *et al*. using infrared spectroscopy following UV irradiation of 2-FA embedded in a cold Ar matrix.[29] The microwave spectrum of 2-FA has never been reported to the best of our knowledge.

In this paper, we report the first microwave spectroscopic study of the lowest energy rotamers of both 2-FA (*anti*) and 3-FA (*syn*). Transitions due to eight heavy atom isotopologues (^{13}C, ^{18}O) of *anti* 2-FA and both *syn* and *anti* rotamers of 3-FA were observed in natural abundance

using high resolution FTMW techniques. The experimental rotational constants determined for the full sets of isotopologues of each species were used to derive the experimental $r_m^{(1)}$ geometries of the anisole backbones of *anti* 2-FA and both *syn* and *anti* 3-FA for comparison with the equilibrium geometries (r_e) calculated at the MP2/cc-pVTZ level. Comparison of the C-C bond lengths in the aromatic ring of each shows a dependence on the orientation of the methoxy group which is consistent with the AGIBA effect as well as the effects of the electron withdrawing fluorine substituent.

EXPERIMENTAL DETAILS

Commercial samples of 2-FA (98%) and 3-FA (99%) were purchased from Sigma-Aldrich Canada and used without further purification. Both samples are liquid at room temperature (mp: -39 ˚C for 2-FA and -35 ˚C for 3-FA) with relatively high boiling points (bp: 154-155 ˚C for 2-FA and 158 ˚C for 3-FA). The samples were placed in glass bubblers individually and neon was used as a carrier gas with a nozzle backing pressure of ~1 atm to deliver detectable quantities of the samples to the spectrometers. The sample mixtures were expanded into the high vacuum chambers of the microwave spectrometers via a supersonic jet expansion using a pulsed nozzle. The rotational spectra of both samples were collected using the chirped pulse FTMW spectrometer and the Balle-Flygare FTMW spectrometer, both of which have been previously described.[30,31]

The broadband spectra were recorded using the chirped pulse FTMW spectrometer in 2 GHz segments from 7 to 19 GHz, and these survey spectra were used to identify the most intense rotational transitions for the parent species and the minor isotopologues (^{13}C and ^{18}O) of the *anti* rotamer of 2-FA and the *syn* and *anti* rotamers of 3-FA. Based on these assignments, the individual rotational transitions were measured in the range of 4-26 GHz using the Balle-Flygare FTMW

spectrometer which affords higher resolution and sensitivity. The spectral lines collected using this cavity based instrument typically have linewidths (fwhm) of ~7 kHz and the frequencies are typically assigned within an uncertainty of ±1 kHz. They are also split into doublets due to the Doppler effect.

COMPUTATIONAL DETAILS

In order to estimate the equilibrium structures, dipole moments and rotational constants, geometry optimization calculations were conducted for anisole as well as both 2-FA and 3-FA using Gaussian 16 software starting from geometries with the heavy atoms of the methoxy group in the plane of the ring and directed toward (*syn*) or away (*anti*) from the fluorine atom. The resulting geometries were verified to be minima from frequency calculations and are summarized in Figure 2. Next, the energy of each compound as a function of the C_2-C_1-O-C_7 dihedral angle was investigated using a series of single point calculations at the MP2/cc-pVTZ level using a step size of 10˚ to convert between the *syn* and *anti* rotamers. At each C_2-C_1-O-C_7 dihedral angle, all other geometric parameters were relaxed. The resulting energy profile for the interconversion between rotamers is plotted in Figure 3.

RESULTS

I. 2-Fluoroanisole (2-FA)

Based on *ab initio* calculations at the MP2/cc-pVTZ level, two rotamers were identified for 2-FA as shown in Figure 2 with the lower energy form being that in which all heavy atoms are in one plane with the methoxy group oriented away (*anti*) from the fluorine substituent. The rotamer that is 6.66 kJ mol^{-1} higher in energy (Figure 3) has the methoxy group turned ~46 degrees

($<C_2$-C_1-O-C_7) out-of-the-plane of the ring from the *syn* position which is not a local minimum. The relative population of the higher energy nonplanar (*np*) rotamer is ~6.8% at room temperature. According to a previous microwave benchmarking study of molecules seeded in a supersonic jet, interconversion barriers greater than 4.8 kJ/mol prevent relaxation between conformers and thus enable observation of transitions due to metastable species even at low rotational temperatures. In this case, however, the barrier to rotate the methoxy group to the *anti* rotamer is lower (4.12 kJ mol^{-1}) and relaxation from the *np* to the *anti* rotamer is anticipated to be facile in the jet.

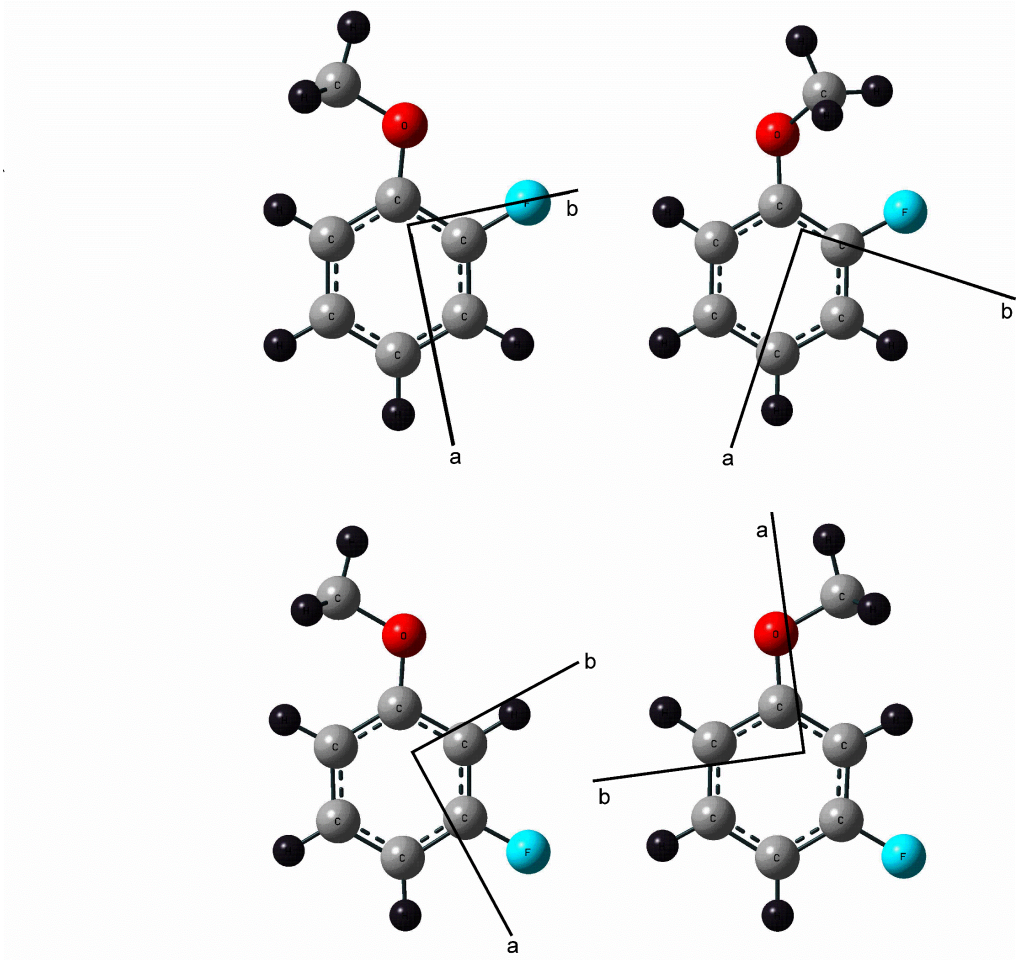

Figure 2: Equilibrium geometries of A) *anti* 2-FA, B) *nonplanar* 2-FA with $<C_2\text{-}C_1\text{-}O\text{-}C_7 = 46^o$, C) *anti* 3-FA and D) *syn* 3-FA in their principal inertial axis systems estimated from MP2/cc-pVTZ calculations.

From analysis of the chirped pulse FTMW spectrum, only transitions related to the *anti* rotamer and its ^{13}C and ^{18}O isotopologues were observed for 2-FA as expected from the energy profile. In total, 46 *a*-type transitions and 153 *b*-type transitions were assigned for the parent isotopologue which is consistent with the dipole moments calculated at the MP2/cc-pVTZ level: $|\mu_a| = 0.47$ D, $|\mu_b| = 2.33$ D, and $|\mu_c| = 0.00$ D. Transitions due to the ^{13}C and ^{18}O isotopologues were also measured but for the latter, only *b*-type transitions were seen due to the low natural

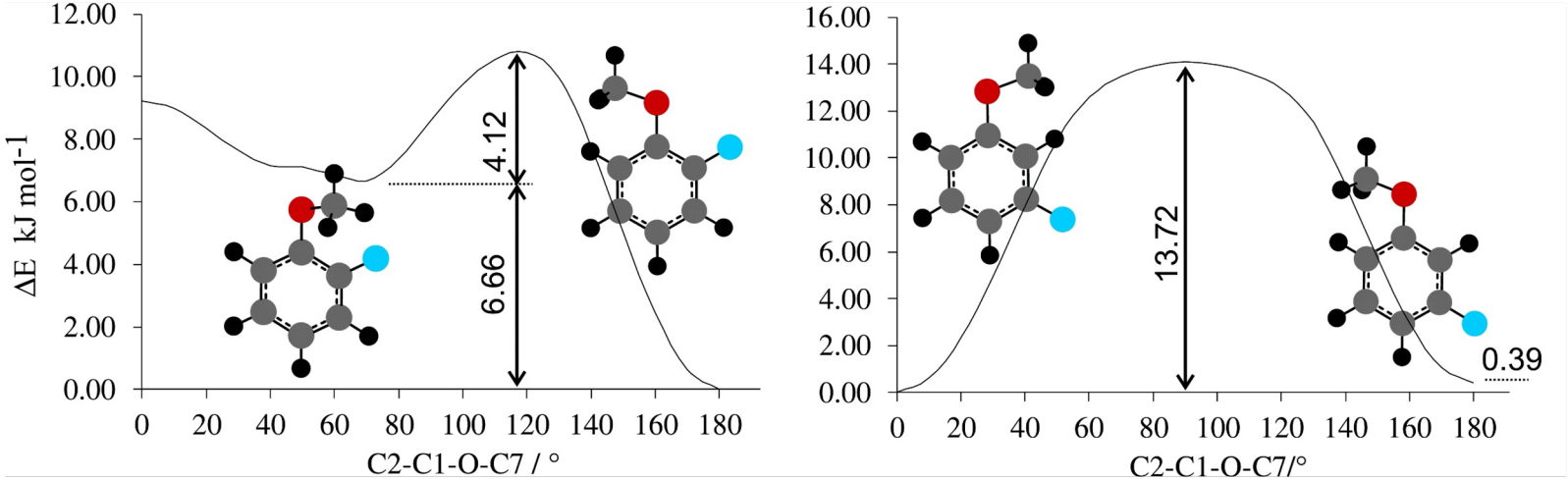

Figure 3: Energy scans (MP2/cc-pVTZ) showing the interconversion path between rotamers of 2-FA and 3-FA.

abundance of ^{18}O (0.2%) and the smaller dipole component along the a-axis. The frequencies corresponding to the observed rotational transitions were fit using Pickett's SPFIT program set to Watson's *A*-reduced Hamiltonian in representation I^r. The rotational and centrifugal distortion constants for *anti* 2-FA are tabulated in Table 1 along with *ab initio* values for comparison. For the minor isotopologues, as fewer transitions were observed overall, Δ_{JK}, Δ_K, δ_J, and δ_K were fixed at the values obtained for the parent species based on the assumption that centrifugal distortion constants do not differ significantly upon isotopic substitution. The rms error of each fit was ~1 kHz, indicating that the Watson Hamiltonian provided a good model for the energy levels of *anti* 2-FA.

II. 3-Fluoroanisole (3-FA)

When the methoxy group is *meta* to fluorine on the ring, the stable rotamers predicted at the MP2/cc-PVTZ level are those that have all heavy atoms in the plane of the ring with the methoxy group either toward (*syn*) or away (*trans*) from fluorine as shown in Figure 2. The energy difference between the *syn* and *anti* rotamers of 3-FA in Figure 3 is predicted to be 0.39 kJ/mol (MP2/cc-pVTZ) suggesting that the proportion of the higher energy *anti* conformation is ~46% at room temperature. The barrier to rotate the methoxy group from the *anti* to *syn* positions is calculated to be 13.33 kJ/mol. Therefore, the *anti* conformation is metastable in the supersonic jet.

In the microwave spectrum of 3-FA, transitions due to both rotamers were readily observed. A portion of the chirped pulse FTMW spectrum is shown in Figure 4. For the parent isotopologue of the *syn* rotamer, 95 *a*-type transitions and 20 *b*-type transitions were recorded. This is consistent with the *ab initio* dipole moments: $|\mu_a| = 1.32$ D, $|\mu_b| = 0.18$ D, and $|\mu_c| = 0.00$ D. Due to the small dipole component along the *b*-axis, no *b*-type transitions were observed for the

heavy atom isotopologues. In the rotational spectrum of *anti* 3-FA, 69 *a*-type transitions and 72 *b*-type transitions were observed. Although *syn* 3-FA is expected to be the dominant rotamer in the jet, the transitions corresponding to the *anti* rotational isomer were nearly twice as intense in Figure 4 due to the greater dipole moments: $|\mu_a| = 2.29$ D, $|\mu_b| = 1.60$ D, and $|\mu_c| = 0.00$ D.

The transitions assigned to each isotopologue of the two rotamers of 3-FA were fit as described above for *anti* 2-FA. For both *syn* and *anti* 3-FA, only the rotational constants and the Δ_J centrifugal distortion constant were determined for the minor isotopologues and the other centrifugal distortion constants were held fixed at the value of the parent isotopologue. The determined spectroscopic constants for *anti* and *syn* 3-FA can be found in Tables 2 and 3, respectively. As with 2-FA, the Watson Hamiltonian provided a good model for these species as indicated by the rms error of ~1 kHz for each fit.

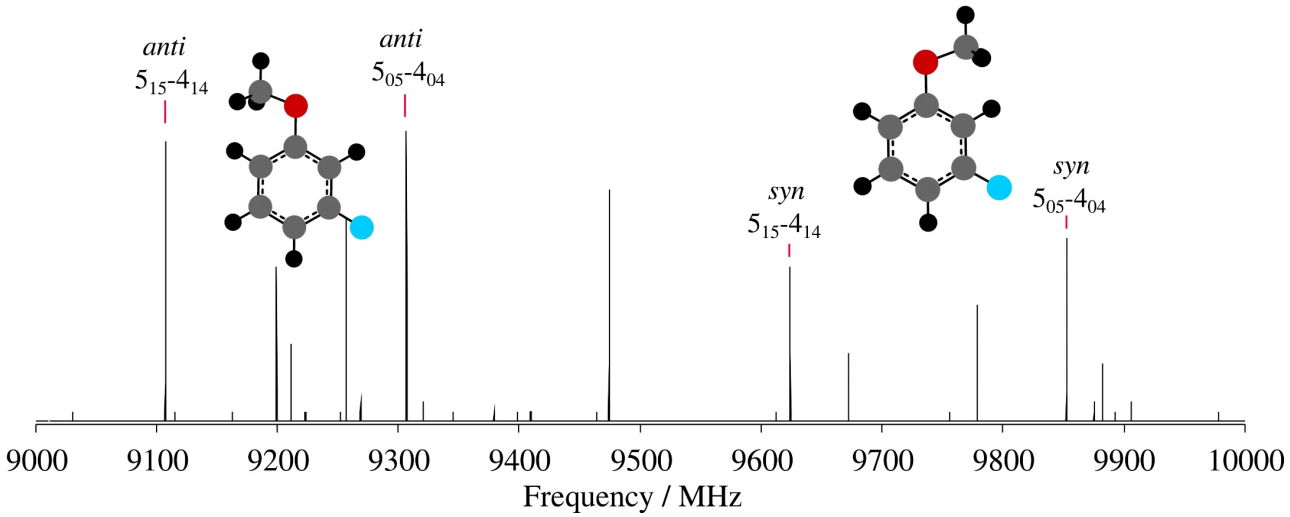

Figure 4: Sample 1 GHz portion of the chirped pulse FTMW spectrum (1.25 million FIDs) of 3-FA showing transitions due to both *anti* and *syn* rotamers. Not all assigned transitions are labelled.

Table 1. Ground State Spectroscopic Constants of *anti* 2-Fluoroanisole Including Its ^{13}C and ^{18}O Isotopologues

	parent	$^{13}C1$	$^{13}C2$	$^{13}C3$	$^{13}C4$	$^{13}C5$	$^{13}C6$	$^{13}C7$	^{18}O
Rotational Constants[a]/MHz									
A	2528.11918(4)	2528.02292(6)	2518.02493(6)	2522.87154(5)	2522.80517(6)	2492.49283(6)	2502.10928(6)	2521.10568(6)	2526.5413(1)
B	1562.84582(2)	1561.74179(5)	1561.90102(5)	1547.18205(4)	1538.47142(7)	1554.03473(6)	1562.87865(5)	1526.56638(6)	1532.73380(9)
C	972.08099(2)	971.64135(5)	970.22060(5)	965.23230(5)	961.82387(5)	963.38719(5)	968.22524(5)	956.91262(5)	960.12582(7)
Centrifugal Distortion Constants[b]/kHz									
Δ_J	0.0537(2)	0.0537(4)	0.0537(4)	0.0526(4)	0.0532(4)	0.0538(4)	0.0534(4)	0.0535(4)	0.0541(5)
Δ_{JK}	0.1071(5)	[0.1071]	[0.1071]	[0.1071]	[0.1071]	[0.1071]	[0.1071]	[0.1071]	[0.1071]
Δ_K	0.1355(5)	[0.1355]	[0.1355]	[0.1355]	[0.1355]	[0.1355]	[0.1355]	[0.1355]	[0.1355]
δ_J	0.01916(7)	[0.01916]	[0.01916]	[0.01916]	[0.01916]	[0.01916]	[0.01916]	[0.01916]	[0.01916]
δ_K	0.1233(4)	[0.1233]	[0.1233]	[0.1233]	[0.1233]	[0.1233]	[0.1233]	[0.1233]	[0.1233]
# lines	199	38	37	41	34	34	36	34	18
rms	0.836	0.974	1.235	1.135	1.493	1.616	1.666	1.195	1.872

[a] Calculated rotational constants (MP2/cc-pVTZ): A=2534.18 MHz, B=1566.12 MHz, C=973.91 MHz.

[b] Calculated centrifugal distortion constants from harmonic frequencies (MP2/cc-pVTZ): Δ_J=0.0524 kHz, Δ_{JK}=0.1239 kHz, Δ_K=0.0940 kHz, δ_J=0.01888 kHz, δ_K=0.1311 kHz.

Table 2. Ground State Spectroscopic Constants of *anti* 3-Fluoroanisole Including Its ^{13}C and ^{18}O Isotopologues

	parent	$^{13}C1$	$^{13}C2$	$^{13}C3$	$^{13}C4$	$^{13}C5$	$^{13}C6$	$^{13}C7$	^{18}O
Rotational Constants[a]/MHz									
A	3615.63732(8)	3614.8509(3)	3592.2220(3)	3613.5027(3)	3585.8255(3)	3531.7594(9)	3578.7190(3)	3614.7755(3)	3575.2464(7)
B	1109.88656(3)	1108.21620(4)	1109.66801(4)	1104.16604(4)	1103.23005(3)	1109.33364(4)	1108.44019(4)	1085.32514(4)	1090.95069(5)
C	854.09682(2)	853.06481(4)	852.65587(4)	850.58718(4)	848.49066(4)	849.00523(5)	851.16794(4)	839.43342(4)	840.62970(6)
Centrifugal Distortion Constants[b]/kHz									
Δ_J	0.0233(1)	0.0232(3)	0.0232(3)	0.0227(2)	0.0228(2)	0.0233(3)	0.0226(3)	0.0222(2)	0.0224(3)
Δ_{JK}	0.0591(5)	[0.0591]	[0.0591]	[0.0591]	[0.0591]	[0.0591]	[0.0591]	[0.0591]	[0.0591]
Δ_K	0.558(6)	[0.0558]	[0.0558]	[0.0558]	[0.0558]	[0.0558]	[0.0558]	[0.0558]	[0.0558]
δ_J	0.00583(4)	[0.00583]	[0.00583]	[0.00583]	[0.00583]	[0.00583]	[0.00583]	[0.00583]	[0.00583]
δ_K	0.082(1)	[0.082]	[0.082]	[0.082]	[0.082]	[0.082]	[0.082]	[0.082]	[0.082]
# lines	141	49	48	50	50	45	48	51	31
rms	0.851	0.810	0.704	0.758	0.652	0.980	0.743	0.761	0.902

[a] Calculated rotational constants (MP2/cc-pVTZ): A=3643.18 MHz, B=1110.29 MHz, C=855.57 MHz.

[b] Calculated centrifugal distortion constants from harmonic frequencies (MP2/cc-pVTZ): Δ_J=0.0224 kHz, Δ_{JK}=0.0611 kHz, Δ_K=0.548 kHz, δ_J=0.00566 kHz, δ_K=0.0835 kHz.

Table 3. Ground State Spectroscopic Constants of *syn* 3-Fluoroanisole Including Its ^{13}C and ^{18}O Isotopologues

	parent	$^{13}C1$	$^{13}C2$	$^{13}C3$	$^{13}C4$	$^{13}C5$	$^{13}C6$	$^{13}C7$	^{18}O
Rotational Constants[a]/MHz									
A	2818.58324(9)	2817.0019(8)	2809.3056(8)	2814.5801(8)	2809.8823(8)	2767.1158(8)	2777.6612(8)	2801.0095(8)	2817.119(1)
B	1281.93939(3)	1279.40902(4)	1282.00212(5)	1276.21328(4)	1270.58226(4)	1278.75946(4)	1281.46063(4)	1256.75761(4)	1250.23084(6)
C	886.37401(3)	885.00843(6)	885.48692(6)	883.23903(6)	880.07893(6)	879.71409(6)	882.05829(6)	872.56400(6)	870.96370(7)
Centrifugal Distortion Constants[b]/kHz									
Δ_J	0.0507(3)	0.0501(4)	0.0499(4)	0.0502(3)	0.0512(3)	0.0498(3)	0.0502(4)	0.0506(4)	0.0486(5)
Δ_{JK}	-0.0931(6)	[-0.0931]	[-0.0931]	[-0.0931]	[-0.0931]	[-0.0931]	[-0.0931]	[-0.0931]	[-0.0931]
Δ_K	0.419(6)	[0.419]	[0.419]	[0.419]	[0.419]	[0.419]	[0.419]	[0.419]	[0.419]
δ_J	0.01781(6)	[0.01781]	[0.01781]	[0.01781]	[0.01781]	[0.01781]	[0.01781]	[0.01781]	[0.01781]
δ_K	0.0804(7)	[0.0804]	[0.0804]	[0.0804]	[0.0804]	[0.0804]	[0.0804]	[0.0804]	[0.0804]
# lines	115	45	45	48	46	50	45	45	24
rms	0.827	1.069	1.212	0.729	1.330	1.245	0.620	1.289	0.833

[a] Calculated rotational constants (MP2/cc-pVTZ): A=2829.77 MHz, B=1283.91 MHz, C=888.17 MHz.

[b] Calculated centrifugal distortion constants from harmonic frequencies (MP2/cc-pVTZ): Δ_J=0.0485 kHz, Δ_{JK}=-0.0629 kHz, Δ_K=0.370 kHz, δ_J=0.0171 kHz, δ_K=0.0882 kHz.

.

III. Structure Determination

With rotational constants from nine isotopologues of each rotamer available, substitution (r_s) structures were first estimated via Kraitchman analysis[2] using Kisiel's KRA program.[32] The absolute values of the Kraitchman coordinates were obtained and their signs were subsequently determined using the *ab initio* geometries as a guide. These parameters are reported in the Supporting Information. The atomic coordinates and their respective Costain errors were then used in the EVAL routine to determine geometric parameters involving the heavy atoms.[32] As in anisole,[21] the geometries of 2-FA and 3-FA using this method were poorly determined. In 2-FA, C6 is sufficiently close to the *b*-axis that its substitution *a*-coordinate is imaginary and appreciable, as is the case for C2 in *syn* 3-FA. Other atoms lying close to an inertial axis also yield large Costain errors and thus, structural parameters involving these atoms were not deemed particularly meaningful.

As 27 rotational constants were determined for each of the three rotamers in Tables 1 through 3, the effective ground state (r_0) structures can be estimated via direct least squares fitting of key geometric parameters to the moments of inertia. The internal coordinates involving the hydrogen and fluorine atoms were fixed at their *ab initio* values during this process. Using this method as incorporated in Kisiel's STRFIT program,[32] we initially found relatively large uncertainties in parameters when all 27 rotational constants were included which mirrored our experience with the fluorobenzaldehydes.[20] While the fluoroanisoles are not strictly planar, the uncertainties of the geometric parameters were reduced when only two rotational constants, for example A and B, were included in the least squares fit but this approach still yielded unsatisfactorily large uncertainties with several bond lengths determined to only about 0.01Å. These results are reported in the Supporting Information.

As reported for anisole,[21] the inclusion of an asymmetric substituent with heavy atoms such as a methoxy group onto the aromatic ring adds out-of-plane vibrational effects that the r_0 approach does

not capture. In such cases, the mass dependence ($r_m^{(1)}$) structure as described by Watson[5] and implemented in STRFIT may provide a better geometric estimate. For each of the three rotamers studied herein, all 27 rotational constants were used to estimate its $r_m^{(1)}$ geometry. The Laurie parameter δ_H was fixed at 0.01 Å for each C-H bond, and the condition that $c_a = c_b = c_c$ was also applied as was reported earlier for anisole.[21] Multiple approaches for defining the Z-matrix of the fluorinated compounds were tested using the earlier results of anisole as an internal check in each case. We report two sets of results in Tables 4 and 5 for anisole, 2-FA and 3-FA and descriptions of each method below.

Under the column heading r_m #1, the Z-matrix was defined as was done previously for six-membered ring compounds such as the fluorinated benzaldehydes,[20] pyridines[15,16] and cyanobenzenes.[17] In this method, nine parameters (five C-C bond lengths and four angles) are needed to define the ring starting from C1, as the remaining distance and angles to close the ring are not independent of these. In this approach, all entries in the Z-matrix correspond to bond lengths and bond angles of the ring with additional geometric parameters that define the methoxy substituent varied or fixed as needed. A second approach we tested was to define the Z-matrix starting from the oxygen of the methoxy group with all other atoms defined relative to this point through the appropriate distances (e.g. C1-O, C2-O) and angles (e.g. C2-O-C1, C3-O-C1) that are not necessarily geometric parameters of the molecule. The results are listed under the r_m #2 heading in Tables 4 and 5. Both methods were test for the anisole parent compound. Comparison of the results obtained by the two methods in Table 4 reveals excellent agreement for all parameters.

Table 4. Equilibrium (r_e) (MP2/aug-cc-pVTZ) and Mass Dependence ($r_m^{(1)}$) Structural Parameters (Bond Lengths in Å, Angles in degrees) Determined for Anisole and 2-Fluoroanisole

	anisole[a]			*anti* 2-fluoroanisole		
	r_e	r_m #1	r_m #2	r_e	r_m #1	r_m #2
C1-C2	1.396	1.385(4)	1.385(4)	1.402	1.401(6)	1.385(6)
C2-C3	1.397	1.409(4)	1.408(4)	1.380	1.379(4)	1.386(2)
C3-C4	1.390	1.391(2)	1.391(2)	1.396	1.399(6)	1.401(4)
C4-C5	1.396	1.398(3)	1.398(3)	1.388	1.392(3)	1.389(3)
C5-C6	1.388	1.392(3)	1.392(3)	1.397	1.414(7)	1.409(5)
C6-C1	1.398	1.397(4)	1.396(4)	1.395	1.385(7)	1.401(7)
C1-O	1.363	1.372(3)	1.372(3)	1.356	1.369(5)	1.361(4)
O-C7	1.416	1.415(2)	1.416(2)	1.418	1.434(3)	1.424(3)
∠(C1-C2-C3)	120.2	118.6(2)	118.7(2)	122.0	122.0(3)	122.3(3)
∠(C2-C3-C4)	120.4	121.0(1)	121.0(1)	119.4	119.2(3)	119.1(2)
∠(C3-C4-C5)	119.3	119.2(1)	119.2(1)	119.6	119.6(1)	119.6(1)
∠(C4-C5-C6)	120.9	120.5(1)	120.5(1)	120.6	120.8(2)	120.8(1)
∠(C5-C6-C1)	119.5	119.4(2)	119.5(2)	120.3	119.2(4)	119.3(3)
∠(C6-C1-C2)	119.8	121.2(3)	121.2(3)	118.0	119.2(4)	118.9(3)
∠(C2-C1-O)	124.5	124.1(3)	124.1(3)	116.1	115.0(5)	116.3(5)
∠(C1-O-C7)	116.3	117.5(2)	117.5(2)	115.9	115.9(3)	117.3(4)

[a] Note that the numbering follows that in Figure 1 for anisole in which the orientation of the methoxy substituent is in the *syn* position by comparison to the fluorinated compounds presented herein.

Table 5. Equilibrium (r_e) (MP2/aug-cc-pVTZ) and Mass Dependence ($r_m^{(1)}$) Structural Parameters (Bond Lengths in Å, Angles in degrees) Determined for Anisole and 2-Fluoroanisole

	anti 3-fluoroanisole			*syn* 3-fluoroanisole		
	r_e	r_m #1	r_m #2	r_e	r_m #1	r_m #2
C1-C2	1.398	1.394(7)	1.395(8)	1.396	1.389(7)	1.395(7)
C2-C3	1.381	1.387(4)	1.387(5)	1.389	1.393(6)	1.388(7)
C3-C4	1.388	1.391(2)	1.390(2)	1.382	1.384(3)	1.380(3)
C4-C5	1.389	1.388(4)	1.387(4)	1.396	1.400(3)	1.400(3)
C5-C6	1.396	1.409(4)	1.411(4)	1.387	1.400(5)	1.404(5)
C6-C1	1.397	1.388(11)	1.387(11)	1.399	1.397(6)	1.396(6)
C1-O	1.360	1.369(6)	1.369(6)	1.359	1.365(3)	1.364(3)
O-C7	1.418	1.419(3)	1.419(3)	1.418	1.424(4)	1.423(4)
∠(C1-C2-C3)	118.8	117.8(4)	117.8(4)	118.2	117.5(3)	117.6(3)
∠(C2-C3-C4)	122.7	123.2(1)	123.2(2)	123.1	123.8(2)	123.9(2)
∠(C3-C4-C5)	117.7	117.4(1)	117.4(1)	117.6	117.2(1)	117.2(1)
∠(C4-C5-C6)	121.4	121.6(1)	121.6(1)	121.1	121.1(2)	121.1(2)
∠(C5-C6-C1)	119.3	118.6(2)	118.6(2)	119.9	119.2(3)	119.1(3)
∠(C6-C1-C2)	120.1	121.4(4)	121.4(4)	120.0	121.2(3)	121.0(4)
∠(C2-C1-O)	115.3	114.2(8)	114.1(8)	124.0	123.8(5)	124.0(5)
∠(C1-O-C7)	116.3	117.4(4)	117.4(4)	116.4	117.3(4)	117.4(4)

DISCUSSION

The ground state spectroscopic constants derived from fitting the observed transitions of the rotamers of 2-FA and 3-FA are well-determined and in good agreement with *ab initio* estimates from MP2/cc-pVTZ calculations as summarized in Tables 1-3. The rotational constants for *anti* 3-FA compare well with those reported by Cervellati *et al.*[27] (A=3615.63(5), B=1109.868(1), C=854.090(1)) but are more precisely determined here using modern FTMW techniques. It is somewhat surprising that the earlier room temperature study included successful observation of pure rotational transitions in three excited torsional states of *trans* 3-FA but failed to assign transitions due to the *syn* rotamer. While *syn* 3-FA is lower in energy by 0.39 kJ mol^{-1}, the dipole moment along the a-axis is only about 60% that of the *anti* analog at the MP2/cc-VTZ level which is presumably the reason this rotamer was not included in the previous study. It is worth noting that the earlier study underestimated the size of the μ_a dipole component to be 0.3 D while our spectra are more consistent with a value of 1.32 D found by *ab initio* methods in the present work.

The $r_m^{(1)}$ geometrical parameters derived from the experimental rotational constants of all three species are summarized in Tables 4 and 5 along with the calculated r_e equilibrium structures (MP2/cc-pVTZ) for comparison. For anisole, both methods of defining the Z-matrix match the structure reported by Desyatnyk *et al.*[21] to within the reported uncertainties. Comparison with the r_e parameters for anisole in the literature (MP2/6-31G(d,p))[21] and from this work (MP2/cc-pVTZ in Table 4) shows satisfactory agreement in most coordinates but minor discrepancies are found in the C1-C2, C2-C3 and C1-O distances which differ by approximately 3σ from the corresponding *ab initio* value. For the rotamers of 3-FA, a similar result is seen with the two sets of experimental parameters (r_m#1 and r_m#2) in full agreement and only a few bond lengths such as C1-O and C5-C6 differing from the r_e value by more than one standard deviation. In *anti* 2-FA, on the other

hand, the two methods of defining the Z-matrix yield parameter sets in which some bond lengths such as C1-C2 and O-C7 differ from each other even when uncertainties are taken into account. Comparison with the r_e structures reveals more discrepancies than for anisole and 3-FA with the greatest deviation seen in the O-C7 distance for which the experimental value differs by 0.016 Å (more than 5σ) using the r_m #1 method. The second approach, however, seems to give improved results for the bond lengths involving O in particular with those matching the r_e counterparts for 2-FA to within 2σ but gives somewhat poorer agreement for C1-C2 and C2-C3 in comparison to the first method. It is unclear why these differences were only an issue for 2-FA as the experimental dataset is robust and more complete than that of *syn* 3-FA for which only *a*-type transitions were measured for the heavy atoms isotopologues. Perhaps this is indicative of a shortcoming in the electronic structure model in capturing the effects of neighboring electron donating (OCH_3) and withdrawing (F) substituents on the ring.

Upon comparing the geometry of anisole with those of 2- and 3-FA in Tables 4 and 5, one can deduce the effect of the electron withdrawing fluorine atom on the ring geometry. One trend is the increase in the C-C-C angle by ~3° at the site of fluorine substitution. The size of this effect is consistent with that reported in earlier FTMW studies of fluorine-substituted benzenes,[12–14] pyridines,[15,16] cyanobenzenes,[17] phenols[18] and thiophenols[19] and is a consequence of the increased p-character in the orbital directed along the C-F bond (and resulting increased s-character in the remaining hybrid orbitals of that carbon center). A second trend that is typically seen is a contraction of the C-C bond lengths (relative to the unsubstituted parent species) on either side of the fluorination site by 0.005 Å to 0.01 Å except in cases where there are compounding effects from two substituents *ortho* to each other as in the difluropyridines[16] and difluorocyanobenzenes.[17] The bond shortening is explained in terms of natural charges on the atoms involved as the electron

withdrawing fluorine induces a positive natural charge on the substituted atom resulting in stronger bonds with the adjacent carbons (C2, C4) that bear partial negative charges. In the present study, a similar reduction in C-C bond lengths is reflected in the bonds involving C3 in 3-FA based on comparison of the r_e and $r_m^{(1)}$ values in Table 5 with those for anisole. This comparison needs to be done with caution, however, as the numbering convention for anisole in Table 4 has the orientation of the methoxy group in the same position as in *syn* 3-FA rotamer. Because of the AGIBA effect in anisole, one must therefore consider the bonds around C5 in anisole when comparing with the bond lengths around C3 in the *anti* 3-FA rotamer. In *anti* 2-FAn, on the other hand, only one of the bonds involving C2 appears to contract according to the r_e and r_m #1 estimates. This is consistent with the calculated values of positive natural charge on C1 (0.243) and C2 (0.370) as a result of the attached electronegative groups at these sites.

It is difficult to separate the effects of the methoxy and fluorine substituents on the ring to deduce whether the former introduces bond length alternation in the ring backbone, the so-called AGIBA effect.[22,23] In anisole itself, bond length alternation was assessed by looking at pairs of bonds across the ring (C2-C3 versus C5-C6, C3-C4 versus C4-C5) and these differed by as much as 0.015 Å (with typical 1σ uncertainty in each bond of ~0.003-0.004 Å).[21] As the presence of fluorine induces additional structural changes in the ring close to its substitution site, this leaves the trio of bonds (C3-C4, C4-C5, C5-C6) in 2-FA as the best candidates from which to assess the effect of the angular methoxy group and one pair of bonds (C4-C5, C5-C6) in the two rotamers of 3-FA. The r_e values in Tables 4 and 5 loosely support the presence of bond length alternation in these compounds with neighbouring bonds differing by 0.007-0.009 Å in these sets. Note, for example, that in *anti* 3-FA, C4-C5 is longer than C5-C6 but the reverse is observed in *syn* 3-FA as depicted via resonance contributors in Figure 5. This is wholly consistent with the presence of the

AGIBA effect as the slightly dominant resonance structure will have the single bond in the O-CH_3 substituent directed away (*anti*) from a single bond in the ring. The experimental $r_m^{(1)}$ geometries appear to capture these trends for the both *anti* rotamers but not for *syn* 3-FA where C4-C5 and C5-C6 are found to be the same. Thus, while FTMW spectroscopy has provided accurate experimental geometries for 2-FA and 3-FA, the AGIBA effect remains a challenge to measure experimentally as the magnitude of bond length alternation falls within typical uncertainties of bond lengths derived from rotational spectra.

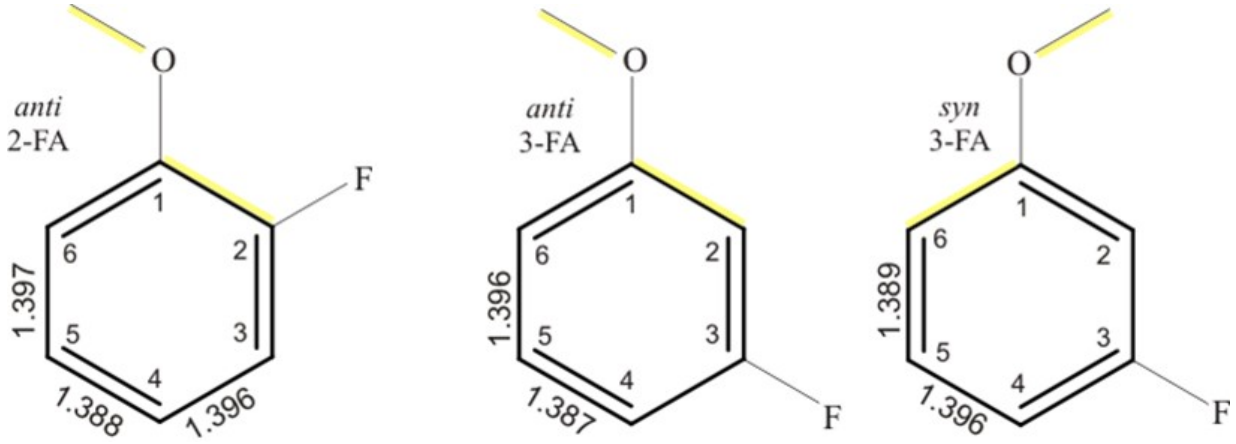

Figure 5: Dominant resonance structures predicted from r_e values (MP2/cc-pVTZ) of 2-FA and 3-FA if the methoxy subsituent induces bond length alternation.

CONCLUSIONS

The rotational spectra of 2-FA and 3-FA were recorded via FTMW spectroscopy and analyzed. This is the first rotational spectroscopic study of 2-FA and is surprisingly the first report of the *syn* rotamer of 3-FA by microwave spectroscopy despite the fact that it is estimated to lie 0.39 kJ mol^{-1} lower in energy than the previously reported *anti* version of this compound. Using the rotational constants from fitting transitions of nine isotopologues of each rotational isomer,

mass dependence $r_m^{(1)}$ structures were derived and the results compare favourably with the *ab initio* r_e geometries at the MP2/cc-pVTZ level. While in anisole, the addition of the angular methoxy group to the ring induces bond length alternation (the so-called AGIBA effect), this pattern is interrupted in 2-FA and 3-FA by the effects of the electron withdrawing fluorine substituent on the ring. As in the anisole parent compound, the geometries for the monofluorinated analogues are generally consistent with the model of unequal resonance contributions in 2-FA and 3-FA with the dominant contributor in each case being the one with the O-CH_3 bond lying *anti* to a single bond in the ring and *syn* to a double bond. While supported by the *ab initio* geometries, comparison of experimental parameters must be performed with caution. This is because the AGIBA effect is predicted to induce bond length alteration of several thousandths of Å which is similar in magnitude to the uncertainties in experimental bond lengths derived from least squares fitting of the moments of inertia.

Acknowledgements

This research is funded by the Natural Sciences and Engineering Research Council of Canada (NSERC) through the Discovery Grant program. KB is grateful for financial support provided through receipt of a NSERC Undergraduate Summer Research Award (USRA). JvW thanks Weslley G. D. P. Silva and Daniel A. Obenchain for useful discussions when preparing the manuscript.

Supporting Information

Appendix I: Equilibrium Structures From MP2/cc-pVTZ Geometry Optimization Calculations For 2-Fluoroanisole, 3-Fluoroanisole and Anisole

Appendix II: Assigned Antiitions for the Isotopologues of 2-Fluoroanisole and 3-Fluoroanisole

Appendix III: Kraitchman Coordinates for 2-Fluoroanisole and 4-Fluoroanisole

Appendix IV: Ground State Effective Structures (r_0)

REFERENCES

(1) Gordy, W.; Cooke, R. L. *Microwave Molecular Spectra*, 3rd ed.; Wiley: New York, 1984.

(2) Kraitchman, J. Determination of Molecular Structure from Microwave Spectroscopic Data. *Am. J. Phys.* **1953**, *21* (1), 17–24.

(3) Nosberger, P.; Bauder, A.; Günthard, H. H. A Versatile Method for Molecular Structure Determinations from Ground State Rotational Constants. *Chem. Phys.* **1973**, *1* (5), 418–425.

(4) Schwendeman, R. H. Structural Parameters from Rotational Spectra. In *Critical Evaluation of Chemical and Physical Structural Information*; Lide, D. R.; Paul, M. A., Ed.; National Academies Press, 1974; pp 94–115.

(5) Watson, J. K. G.; Roytburg, A.; Ulrich, W. Least-Squares Mass-Dependence Molecular Structures. *J. Mol. Spectrosc.* **1999**, *196* (1), 102–119.

(6) Leung, H. O.; Marshall, M. D. Exploring the Forces Contributing to Noncovalent Bonding by Microwave Spectroscopy and Structural Characterization of Gas-Phase Heterodimers of Protic Acids with Haloethylenes. *J. Phys. Chem. A* **2019**, *123*, 10846–10861.

(7) Lu, T.; Chen, J.; Zhang, J.; Gou, Q.; Xia, Z.; Feng, G. Conformational Landscape of the Weakly Bound Difluoromethane–1,1-Difluoroethane Dimer Explored by Rotational Spectroscopy and Quantum Chemical Calculations. *J. Mol. Spectrosc.* **2019**, *357*, 32–37.

(8) Zhang, J.; Ye, H.; Jin, Y.; Gou, Q.; Biczysko, M.; Feng, G. Conformational Equilibria and Molecular Structures of Model Sulfur-Sulfur Bridge Systems: Diisopropyl Disulfide. *J.*

Phys. Chem. A **2019**, *123*, 10714–10720.

(9) Carlson, C. D.; Seifert, N. A.; Heger, M.; Xie, F.; Thomas, J.; Xu, Y. Conformational Dynamics of 1-Phenyl-2,2,2-Trifluoroethanol by Rotational Spectroscopy and Ab Initio Calculations. *J. Mol. Spectrosc.* **2018**, *351*, 62–67.

(10) Nair, K. P. R.; Herbers, S.; Grabow, J. U. Structure and Methyl Torsion of Halogenated Toluenes: Rotational Spectrum of 3,4-Difluorotoluene. *J. Mol. Spectrosc.* **2019**, *355*, 19–25.

(11) Herbers, S.; Wachsmuth, D.; Obenchain, D. A.; Grabow, J. U. Rotational Characterization of Methyl Methacrylate: Internal Dynamics and Structure Determination. *J. Mol. Spectrosc.* **2018**, *343*, 96–101.

(12) Kisiel, Z.; Białkowska-Jaworska, E.; Pszczółkowski, L. The Millimeter-Wave Rotational Spectrum of Fluorobenzene. *J. Mol. Spectrosc.* **2005**, *232* (1), 47–54.

(13) Nygaard, L.; Bojesen, I.; Pedersen, T.; Rastrup-Andersen, J. Structure of Fluorobenzene. *J. Mol. Struct.* **1968**, *2* (3), 209–215.

(14) Doraiswamy, S.; Sharma, S. D. R0 Geometries of Fluorobenzenes and Distortions in Benzene Ring Structure on Substitution. *J. Mol. Struct.* **1983**, *102* (1–2), 81–92.

(15) van Dijk, C. W. C. W.; Sun, M.; van Wijngaarden, J. Microwave Rotational Spectra and Structures of 2-Fluoropyridine and 3-Fluoropyridine. *J. Phys. Chem. A* **2012**, *116* (16), 4082–4088.

(16) van Dijk, C. W. C. W.; Sun, M.; van Wijngaarden, J. Investigation of Structural Trends in Difluoropyridine Rings Using Chirped-Pulse Fourier Transform Microwave Spectroscopy and Ab Initio Calculations. *J. Mol. Spectrosc.* **2012**, *280* (1), 34–41.

(17) Kamaee, M.; Sun, M.; Luong, H.; van Wijngaarden, J. Investigation of Structural Trends

in Mono-, Di-, and Pentafluorobenzonitriles Using Fourier Transform Microwave Spectroscopy. *J. Phys. Chem. A* **2015**, *119* (41), 10279–10292.

(18) Bell, A.; Singer, J.; Desmond, D.; Mahassneh, O.; van Wijngaarden, J. Rotational Spectra and Conformer Geometries of 2-Fluorophenol and 3-Fluorophenol. *J. Mol. Spectrosc.* **2017**, *331*, 53–59.

(19) Sun, W.; van Wijngaarden, J. Structural Elucidation of 2-Fluorothiophenol from Fourier Transform Microwave Spectra and Ab Initio Calculations. *J. Mol. Struct.* **2017**, *1144*, 496–501.

(20) Sun, W.; Lozada, I. B.; Van Wijngaarden, J. Fourier Transform Microwave Spectroscopic and Ab Initio Study of the Rotamers of 2-Fluorobenzaldehyde and 3-Fluorobenzaldehyde. *J. Phys. Chem. A* **2018**, *122* (8), 2060–2068.

(21) Desyatnyk, O.; Pszczółkowski, L.; Thorwirth, S.; Krygowski, T. M.; Kisiel, Z. The Rotational Spectra, Electric Dipole Moments and Molecular Structures of Anisole and Benzaldehyde. *Phys. Chem. Chem. Phys.* **2005**, *7* (8), 1708–1715.

(22) Krygowski, T. M.; Cyrański, M. K. Angular Group Induced Bond Alternation (AGIBA). A New Face of Substituent Effect Detected in Molecular Geometry. *Synlett* **2003**, *2003* (07), 922–936.

(23) Krygowski, T. M.; Wisiorowski, M.; Howard, S. T.; Stolarczyk, L. Z. Angular-Group-Induced Bond Alternation. I. Origin of the Effect from Ab Initio Calculations. *Tetrahedron* **1997**, *53* (38), 13027–13036.

(24) Owen, N. L.; Hester, R. E. Vibrational Spectra and Torsional Barriers of Anisole and Some Monohalogen Derivatives. *Spectrochim. Acta* **1969**, *25A*, 343–354.

(25) Schaefer, T.; Sebastian, R. 1H Nuclear Magnetic Resonance and Molecular Orbital

Studies of the Conformations of 3-Fluoroanisole. *Can. J. Chem.* **1989**, *67* (4), 1027–1031.

(26) Dorofeeva, O. V.; Vishnevskiy, Y. V.; Rykov, A. N.; Karasev, N. M.; Moiseeva, N. F.; Vilkov, L. V.; Oberhammer, H. Molecular Structure, Conformation, Potential to Internal Rotation, and Ideal Gas Thermodynamic Properties of 3-Fluoroanisole and 3 , 5-Difluoroanisole as Studied by Gas-Phase Electron Diffraction and Quantum Chemical Calculations. **2006**, *789*, 100–111.

(27) Cervellati, R.; Lister, D. G.; Christen, D.; Hoffmann, V. The Microwave Spectrum and Methoxy Torsional Frequency of the Anti Rotamer of M-Fluoroanisole. *J. Mol. Struct.* **1982**, *82*, 307–309.

(28) Novikov, V. P.; Vilkov, L. V; Oberhammer, H. Conformational Properties of 2-Fluoroanisole in the Gas Phase. **2003**, 908–913.

(29) Isozaki, T.; Sakeda, K.; Suzuki, T.; Ichimura, T. Evidence for a Non-Planar Conformer and Conformational Isomerization of o -Fluoroanisole in a Low-Temperature Ar Matrix. **2005**, *409*, 93–97.

(30) Sedo, G.; van Wijngaarden, J. Fourier Transform Microwave Spectra of a New Isomer of OCS- CO2. *J. Chem. Phys.* **2009**, *131* (4), 044303.

(31) Evangelisti, L.; Sedo, G.; van Wijngaarden, J. Rotational Spectrum of 1,1,1-Trifluoro-2-Butanone Using Chirped-Pulse Fourier Transform Microwave Spectroscopy. *J. Phys. Chem. A* **2011**, *115* (5).

(32) Kisiel, Z. PROSPE http://www.ifpan.edu.pl/~kisiel/prospe.htm (accessed Dec 3, 2019).

TOC Graphic